Titanium Complexes of Oxacalix[3]arenes: Synthesis and Mechanistic Studies of Their Dynamic Isomerization

Philip D. Hampton,* Charles E. Daitch, Todd M. Alam, Zsolt Bencze, and Melanie Rosay

Department of Chemistry, University of New Mexico, Albuquerque, New Mexico 87131-1096

Received November 4, 1993[⊗]

The coordination chemistry of oxacalix[3]arenes with Ti(IV) has been examined. Several Ti(L)X complexes have been prepared and characterized where L represents the trianion of the oxacalix[3]arene macrocycle and X is an isopropoxide or acetylacetonate (acac) ligand. The Ti(L)(acac) complex exhibits a dynamic interconversion on the ^{1}H NMR time scale. At room temperature, the macrocycle ligand in the complex exhibits C_{3v} symmetry and the acac methyls are equivalent. In contrast, at low temperatures, the macrocycle possesses C_s symmetry and the acac methyls are inequivalent. Computer simulation of variable temperature NMR experiments have provided rate constants and activation parameters for the interconversion process. Rapid isomerization of trigonal bipyramidal isomers via turnstile rotation or Berry pseudorotation processes is proposed to explain the dynamic behavior of this complex.

Introduction

Calixarenes have received considerable attention for their host−guest chemistry, their ability to bind main group metals, and their complexation of transition metals.[1−3] In contrast, there have been no reports of the ability of the hexahomotrioxacalix[3]arene macrocycles **1**, abbreviated oxacalix[3]arenes in this paper, to bind transition metals, and only a few reports of their ability to bind main group metals.[4,5] The low yields and difficult purification reported in the literature for the *tert*-butyloxacalix[3]arene macrocycle **1** (R = *t*-Bu) is probably the reason why the macrocycles have not received attention as ligands for metals.[6,7] We recently reported a new synthesis of the oxacalix[3]arenes **1** that provides the macrocycles in good yields.[5] With this improved synthesis, it is now possible to study the transition-metal complexing ability of these interesting macrocycles.

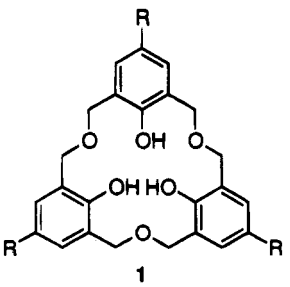

1

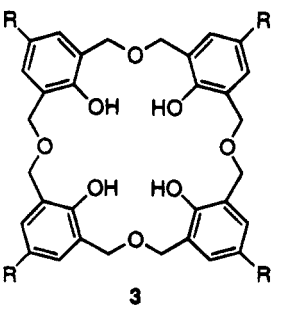

3

Our new synthesis of the oxacalix[3]arenes **1** (R = *t*-Bu, *i*-Pr, Et, Me, and Cl) involves a high-dilution, acid-catalyzed condensation of the 2,6-bis(hydroxymethyl)phenols **2** to yield a mixture of oxacalix[3]arene **1** and oxacalix[4]arene **3**, as shown in eq 1. The mixture of **1** and **3** can be separated through the precipitation of the oxacalix[3]arenes **1** as the sodium or potassium salts of their monoanions, followed by protonation of the isolated salts. This synthesis provides the macrocycles in high purity with yields of up to 30%. Oxacalix[3]arenes **1** (R = *i*-Pr, Et, Me, and Cl) are new macrocycles.[5]

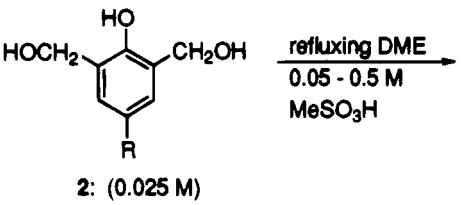

2: (0.025 M)

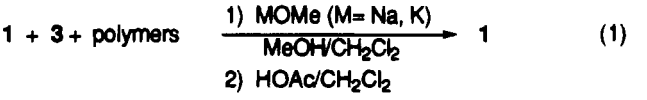

(1)

In this paper, we describe the synthesis of the titanium(IV) complexes **4** and **5** of oxacalix[3]arene **1** (R = *t*-Bu), where the macrocycle is a trianionic ligand to the titanium center. The trianion of macrocycle **1** (R = *t*-Bu) will be abbreviated as L.

Experimental Section

General Conditions. All solvents were dried using either calcium hydride or sodium benzophenone ketyl and degassed. 2,4-Pentanedione was distilled under reduced pressure, degassed, and dried over 3 Å molecular sieves. The titanium complexes were prepared and handled under inert atmosphere using either Schlenk or drybox techniques.

NMR spectra were recorded on a Bruker AC-250 at resonant frequencies of 250 and 62.9 MHz for ^{1}H and ^{13}C, respectively. Chemical shifts were referenced to either tetramethylsilane or protio solvent impurity. Attached proton test experiments were carried out on ^{13}C NMR spectra so that negative peaks [APT(−)] and positive

[⊗] Abstract published in *Advance ACS Abstracts,* September 1, 1994.

(1) For reviews of calixarenes, see: (a) Gutsche, C. D. *Prog. Macrocyclic Chem.* **1987**, *3*, 93−165. (b) Gutsche, C. D. *Calixarenes*; Royal Society of Chemistry: Cambridge, England, 1989. (c) *Calixarenes: A Versatile Class of Macrocyclic Compounds*; Vicens, J., Böhmer, V., Eds.; Kluwer: Dordrecht, The Netherlands, 1991.

(2) For a discussion of the ability of calixarenes to bind main group metals, see: (a) Chang, S.; Cho, I. *J. Chem. Soc. Perkin Trans. I* **1986**, 211. (b) Iwamoto, K.; Shinkai, S. *J. Org. Chem.* **1992**, *57*, 7066.

(3) For a discussion of transition metal complexes of calixarenes, see: (a) Bott, S. G.; Coleman, A. W.; Atwood, J. L. *Chem. Commun.* **1986**, 610. (b) Olmstead, M. M.; Sigel, G.; Hope, H.; Xu, X.; Power, P. P. *J. Am. Chem. Soc.* **1985**, *107*, 8087. (c) Asfari, Z.; Harrowfield, J. M.; Ogden, M. I.; Vicens, J.; White, A. H. *Angew. Chem., Int. Ed. Engl.* **1991**, *30*, 854. (d) Xu, B.; Swager, T. M. *J. Am. Chem. Soc.* **1993**, *115*, 1159.

(4) (a) Araki, K.; Hashimoto, N.; Otsuka, H.; Shinkai, S. *J. Org. Chem.* **1993**, *58*, 5958. (b) Araki, K.; Inada, K.; Otsuka, H.; Shinkai, S. *Tetrahedron* **1993**, *49*, 9465.

(5) Hampton, P. D.; Bencze, Z.; Tong, W.; Daitch, C. E. *J. Org. Chem.*, in press.

(6) Zerr, P.; Mussrabi, M.; Vicens, J. *Tetrahedron Lett.* **1991**, *32*, 1879.

(7) Dhawan, B.; Gutsche, C. D. *J. Org. Chem.* **1983**, *48*, 1536.

0020-1669/94/1333-4750$04.50/0

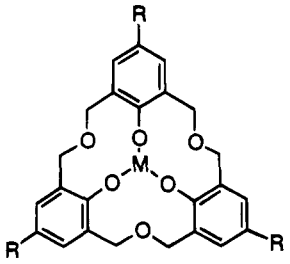

4a: M= Ti(O*i*-Pr)
4b: M= Ti(O*i*-Pr)$_2$
5: M= Ti(acac)

peaks [APT(+)] corresponded to carbon atoms possessing an even and odd number of hydrogens, respectively. Elemental analyses were performed by Galbraith Laboratories.

[Ti(L)(isopropoxide)]$_n$ (4). In an inert atmosphere glovebox, a solution of 28.4 mg Ti(O-*i*-Pr)$_4$ (0.10 mmol) in 10 mL of methylene chloride was added to a solution of 58.0 mg of macrocycle **1** (R = *t*-Bu) (0.10 mmol) in 10 mL of methylene chloride. The macrocycle solution immediately turned yellow on addition of Ti(O-*i*-Pr)$_4$. After stirring for an hour under inert atmosphere, the solvent was removed *in vacuo*. The resulting solid was dried overnight *in vacuo*. ^{1}H NMR ($CDCl_3$): δ 7.15 (s, 6H, 3,5-aryl protons), 5.25 and 5.04 (pair of d, J = 9.0 and 9.8 Hz, respectively, combined integration 6H, macrocycle methylene protons), 4.44 and 4.30 (pair of d, J = 9.8 and 9.0 Hz, respectively, combined integration 6H, macrocycle methylene protons), 3.50 (m, 1H, J = 6.2 Hz, OC*H*$(CH_3)_2$), 1.22 (s, 27 H, C(C*H*$_3)_3$), and −0.16 (d, J = 6.2 Hz, 6H, OCH(C*H*$_3)_2$). Note: the complex is a mixture of two species which are in a ratio that varies from batch to batch. Typical ratios of the major species (upfield and downfield doublets) to the minor species (central doublets) ranged from 2.2:1 to 8.6:1. Addition of THF to the mixture in $CDCl_3$ resulted in a simplification of the methylene region to a single pair of doublets: δ 7.12 (s, 6H, 3,5-aryl protons), 4.80 (d, J = 8.7 Hz, 6H, macrocycle methylene protons) and 4.28 (s, J = 8.8 Hz, 6H, macrocycle methylene protons), 1.16 (27 H, *tert*-butyl protons), and −0.21 (d, J = 6.2 Hz, 6H, OCH(C*H*$_3)_2$). Note: the *i*-Pr methine signal of this compound was probably masked by the THF signals.

[Ti(L)(acetylacetonate)] (5). In an inert atmosphere glovebox, a solution of 103 mg (0.35 mmol) of Ti(O-*i*-Pr)$_4$ in 20 mL of CH_2Cl_2 was added to a solution of 202 mg (0.35 mmol) of macrocycle **1** (R = *t*-Bu) in 20 mL of CH_2Cl_2, and the reaction mixture was stirred for 2 h. The solvent was removed *in vacuo*. The yellow solid was dissolved in 20 mL of THF, and 34.8 mg (0.35 mmol) of 2,4-pentanedione was added. The color immediately changed from yellow to orange. After 1 h, the solvent was removed. The orange solid was recrystallized from hot hexane. Yield: 90%. ^{1}H NMR (CD_2Cl_2, 298 K): δ 7.23 (s, 6H, macrocycle 3,5-aryl protons), 5.88 (s, 1H, acac methine proton), 4.77 (d, J = 10.0 Hz, 6H, macrocycle methylene protons), 4.42 (d, J = 10.0 Hz, 6H, macrocycle methylene protons), 1.91 (s, 6H, acac methyl protons), 1.28 (s, 27H, *tert*-butyl protons). ^{1}H NMR (CD_2Cl_2, 182 K): δ 7.29 (s, 2H, 3,5-aryl protons), 7.19 (s, 4H, 3,5-aryl protons), 5.87 (s, 1H, acac methine), 5.11 (d, J = 10.1 Hz, 2H, macrocycle methylene, H_1), 4.84 (d, J = 13.0 Hz, 2H, macrocycle methylene, H_2), 4.62 (d, J = 10.1 Hz, 2H, macrocycle methylene, $H_{1'}$), 4.26 and 4.24 (overlapping d, J = 11.3 and 13.0 Hz, 4H, macrocycle methylene, $H_{3'}$ and $H_{2'}$, respectively), 3.96 (d, J = 11.3 Hz, 2H, macrocycle methylene, H_3), 2.09 (s, 3H, acac methyl, H_4), 1.39 (s, 3H, acac methyl, H_5), and 1.20 (s, 27H, C(C*H*$_3)_3$). ^{13}C NMR ($CDCl_3$, 298 K): δ 191.74 (2C, APT(−), acac carbonyl), 163.67 (3C, APT(−), macrocycle 1-aryl), 143.39 (3C, APT(−), macrocycle 4-aryl), 127.20 (6C, APT(+), macrocycle 3,5-aryl), 125.21 (6C, APT(−), macrocycle 2,6-aryl), 106.14 (1C, APT(+), acac methine), 70.42 (6C, APT(−), macrocycle *C*H_2), 34.38 (3C, APT(−), *C*$(CH_3)_3$), 31.67 (9C, APT(+), C(*C*$H_3)_3$), and 26.00 (2C, APT(+), acac methyls). ^{13}C NMR ($CDCl_3$, 182 K): δ 192.59 (1C, acac carbonyl), 189.80 (1C, acac carbonyl), 163.18 (2C, macrocycle 1-aryl), 161.98 (1C, macrocycle 1-aryl), 142.74 (2C, macrocycle 4-aryl), 141.89 (1C, macrocycle 4-aryl), 126.64 (4C, macrocycle 3,5-aryl), 125.47 (2C, macrocycle 3,5-aryl), 124.24 (2C, macrocycle 2,6-aryl), 123.45 (2C, macrocycle 2,6-aryl), 122.84 (2C, macrocycle 2,6-aryl), 106.76 (1C, acac methine), 70.89 (2C, macrocycle *C*H_2), 67.35 (2C, macrocycle *C*H_2), 65.75 (2C, macrocycle *C*H_2), 33.62 (3C, *C*$(CH_3)_3$), 30.71 (9C, C(*C*$H_3)_3$), 25.51 (1C, acac methyl), and 25.12 (1C, acac methyl). UV−visible: λ (ϵ) 338 nm (7940 M^{-1} cm^{-1}). FTIR (KBr): ν 2957, 2904, 2866, 1580, 1530, 1478, 1356, 1281, 1219, 1123, 1069, 1032, 937, 880, 847, 785, 671, 571, 473 cm^{-1}. FTIR (cyclohexane): ν 2940, 2922, 2906, 2868, 1589, 1529, 1477, 1361, 1311, 1282, 1219, 1079, 879, 848, 783, 571 cm^{-1}. Anal. Calcd for $C_{41}H_{52}O_8Ti$: C, 68.32; H, 7.27; Ti, 6.65. Found: C, 68.28; H, 7.55; Ti, 6.70. LRFAB (*o*-nitrophenyl octyl ether matrix): calcd for $C_{41}H_{52}O_8Ti$, *m/z* (M^+) 718.3 (^{46}Ti, 7%), 719.3 (^{47}Ti, 14%), 720.3 (^{48}Ti, 100%), 721.3 (^{49}Ti, 53%), 722.3 (^{50}Ti, 22%), 723.3 (^{50}Ti, ^{13}C, 7%), and $(M + H)^+$ 719.3 (^{46}Ti, 10%), 720.3 (^{47}Ti, 14%), 721.3 (^{48}Ti, 100%), 722.3 (^{49}Ti, 53%), 723.3 (^{50}Ti, 22%), and 724.3 (^{50}Ti, ^{13}C, 7%); found, *m/z* 718.4 [$(M^+)(^{46}Ti)$, 13%], 719.5 [$(M^+)(^{47}Ti)$ and $(M + H^+)(^{46}Ti)$, 29%], 720.5 [$(M^+)(^{48}Ti)$ and $(M + H^+)(^{47}Ti)$, 90%], 721.5 [$(M^+)(^{49}Ti)$ and $(M + H^+)(^{48}Ti)$, 100%], 722.5 [$(M^+)(^{50}Ti)$ and $(M + H^+)(^{49}Ti)$, 52%], 723.5 [$(M + H^+)(^{50}Ti)$, 23%], and 724.6 [$(M + H^+)(^{50}Ti, ^{13}C)$, 23%].

Chart 1. Atom Labeling Diagram for the Macrocycle Ligand

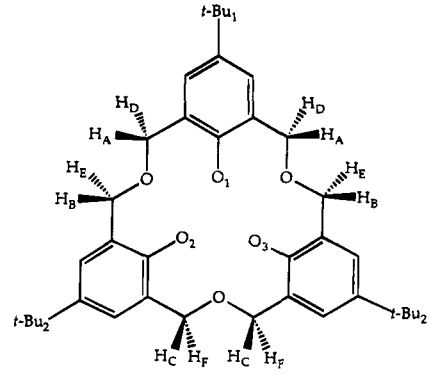

Variable Temperature ^{1}H NMR Experiments. Variable temperature ^{1}H NMR spectra were the result of 32 scans, using 16K complex points, a spectral width of 3250 Hz, and a total acquisition time of 8 s (3 s relaxation delay) at 5 K intervals over the temperature range 182−310 K in CD_2Cl_2. Temperature control was accurate to ± 1 K and was previously calibrated using an external reference. Following transformation and phasing, spectra were transferred to a PC using ZZNET.[8] No change was observed in the spectra or lineshapes when the concentration of complex **5** was increased by a factor of 4.7.

Simulation of Variable Temperature ^{1}H NMR Spectra. Before the acac methyl and macrocycle methylene regions could be simulated, it was necessary to determine which of the methylene protons were attached to the same carbon atom (H_1 and $H_{1'}$, H_2 and $H_{2'}$, H_3 and $H_{3'}$) and which set of three protons were on the same face of the macrocycle (H_1, H_2, and H_3; $H_{1'}$, $H_{2'}$, and $H_{3'}$). The pairings of H_i with $H_{i'}$ (i = 1−3) for protons attached to the same carbon atom, were determined based on the coupling constants for the six doublets in the low temperature ^{1}H NMR spectrum ($J_{11'}$ = 10.1 Hz, $J_{22'}$ = 13.0 Hz, and $J_{33'}$ = 11.3 Hz). The protons on the same face of the macrocycle were determined based upon the observed independent coalescence of the sets of H_i and $H_{i'}$ doublets as the temperature was raised.

Assignment of the H_i or $H_{i'}$ protons to protons H_A−H_F on the macrocycle ligand (Chart 1) was not possible. The actual assignments of the protons is not necessary for the simulation of the spectra, since the exchanges between the protons are correlated. The methylene region exhibited a pair of doublets up to 329 K. Thus, no exchange is observed between the H_i and $H_{i'}$ sets of protons. It was also not possible to determine which set of protons, H_i or $H_{i'}$, were on the same face of the macrocycle as the titanium center. No signal enhancement was observed by NOE at 310 K for either of the methylene doublets on irradiation of the acac methyl singlet.

The temperature dependence of the chemical shift, J coupling, and relaxation rates (R_2) in the intermediate exchange region were estimated

(8) Zolani, Z.; Westler, W. M.; Ulrich, E. L.; Markley, J. L. *J. Magn. Reson.* **1990**, *88*, 511.

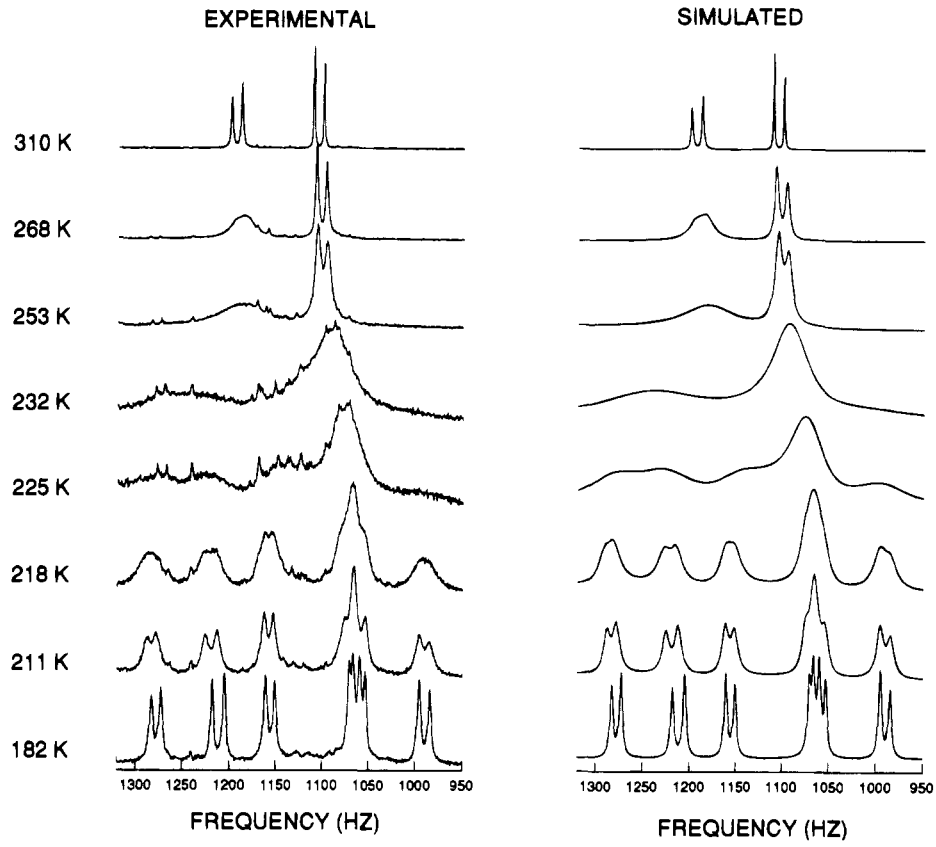

Figure 1. Variable temperature ^{1}H NMR spectra for the macrocycle methylene region of complex **5** (left, experimental spectra; right, simulated spectra).

using an extrapolation from the low temperature behavior. In the low temperature region, the exchange rates are assumed to be slow in comparison to the frequency separation between exchanging resonances, thus the line shapes are not affected by exchange. The temperature dependence of the chemical shifts (ν_{cs}) of the six doublets was initially estimated using a linear dependence, but it was discovered that a second-order fit described the temperature dependence of the chemical shift of H_1 [$\nu_{cs}(H_1)$] more accurately (eq 2). Second-order temperature dependence of chemical shift is a precedented phenomenon.[9] Equations 2−9 describe the temperature dependence of the chemical shifts (ν_{cs}) in Hz for the macrocycle methylene protons H_i and $H_{i'}$ ($i = 1-3$) and the acac methyl protons H_4 and H_5 as a function of temperature in K. All the $^2J_{HH}$ coupling constants and relaxation rates were found to be invariant with temperature over the range investigated.

$$\nu_{cs}(H_1) = (7.85 \times 10^{-3})T^2 + (-2.91)T + 1.55 \times 10^3 \quad (2)$$

$$\nu_{cs}(H_{1'}) = 0.042T + 1.15 \times 10^3 \quad (3)$$

$$\nu_{cs}(H_2) = 0.26T + 1.16 \times 10^3 \quad (4)$$

$$\nu_{cs}(H_{2'}) = 1060 \quad (5)$$

$$\nu_{cs}(H_3) = 990 \quad (6)$$

$$\nu_{cs}(H_{3'}) = 0.188T + 1.03 \times 10^3 \quad (7)$$

$$\nu_{cs}(H_4) = 0.206T + 309 \quad (8)$$

$$\nu_{cs}(H_5) = 0.186T + 488 \quad (9)$$

Simulations of experimental variable temperature data for the acac methyl and macrocycle methylene regions were obtained using a modified version of DNMR5.[10] Kinetic matrices for the simulation of these regions are provided in the supplementary material. The series of spectra on the left side of Figure 1 were fit to the two independent

Scheme 1. Proposed Mechanism for the Exchange of the Macrocycle Methylene Protons

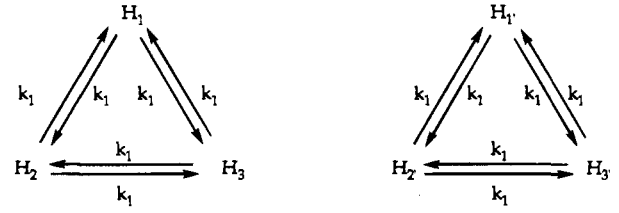

three-site exchange processes shown in Scheme 1. Only the rate constant k_1 was simulated using DNMR5, since the H_i and $H_{i'}$ sets of protons are in equal populations due to their presence in a single macrocycle ligand.

The acac methyl region of the ^{1}H NMR spectrum shown on the left side of Figure 2 was initially simulated by the two-site exchange process indicated in Scheme 2A. In this process, k_2 is the rate constant for exchange between the two inequivalent acac methyl groups, designated as H_4 and H_5 in Scheme 2A for the downfield and upfield singlets, respectively. Attempts to fit this simple two-site exchange process to the experimental spectra in Figure 2 were not successful due to three factors: (1) the downfield signal had a greater integral at low temperatures (~4%), (2) the two singlets exhibited differential broadening, and (3) the high temperature singlet was shifted significantly downfield from the midpoint between the low temperature singlets. The integrals were unaffected when the relaxation delay was increased to 20 s; thus, the different integrals for the upfield and downfield signals are not due to an incomplete relaxation of the acac methyl groups.

Two alternative mechanisms (parts B and C of Scheme 2) were then examined for simulation of the acac methyl region. Both mechanisms

(9) Sandström, J. *Dynamic NMR Spectroscopy*; Academic: London, 1982; pp 86−87.
(10) Stephenson, D. S.; Binsch, G., 1978, DNMR5. Quantum Chemistry Program Exchange, Indiana University, Bloomington, IN 47405; Program 365.

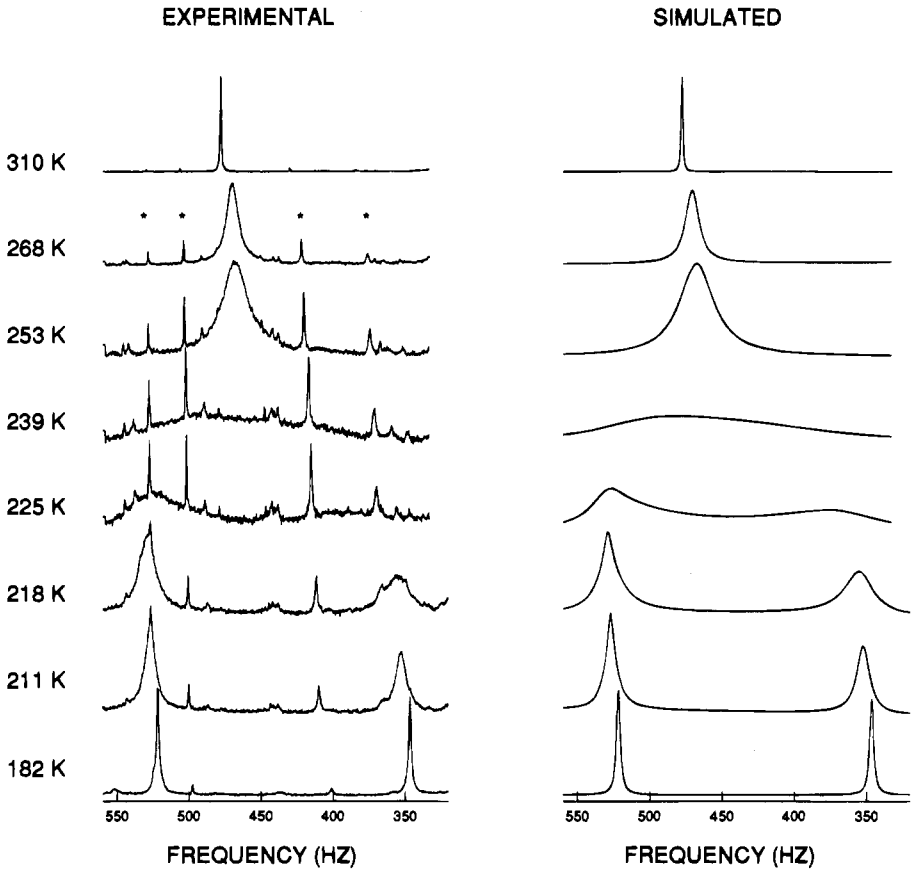

Figure 2. Variable temperature ^{1}H NMR spectra for the acac methyl region of complex **5** (left, experimental spectra; right, simulated spectra).

Scheme 2. Proposed Mechanisms for the Exchange of the Acac Methyl Protons

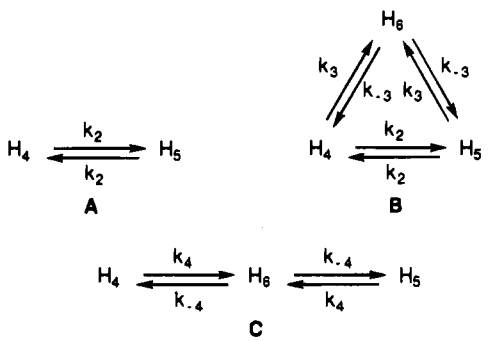

included a minor isomer that possesses a single acac methyl ^{1}H NMR signal (H_6) that lies under the downfield singlet, and whose concentration is temperature dependent. In the first mechanism (Scheme 2B), the proton sites on the major species (H_4 and H_5) are in equilibrium with one another and with the minor species (H_6). In the simulation, the program fit the experimental spectra by varying k_2 and k_3, and the population of the minor reaction component. The value of k_{-3} is not directly simulated, but it could be calculated using values for k_3 and the population of the minor isomer.

The mechanism in Scheme 2C is similar to that in Scheme 2B, except that the proton sites on the major species (H_4 and H_5) do not directly exchange with one another, but they exchange via their conversion to the single proton site on the minor species (H_6). In this simulation, the concentration of the minor species obtained from the above simulation of Scheme 2B were used, and only the value of k_4 was varied by DNMR5. The simulated spectra obtained from this simulation were identical to those obtained for Scheme 2C.

Results

Synthesis and Characterization of Titanium(IV) Complexes of Oxacalix[3]arene 1 (R = *t*-Bu). Reaction of macrocycle **1** (R = *t*-Bu) with 1 equiv of titanium(IV) isopropoxide in methylene chloride results in rapid formation of a yellow solution from which a yellow solid can be isolated on removal of the solvent. In contrast to the NMR spectrum for the macrocycle which possesses equivalent methylene protons on the two faces of the macrocycle, the titanium complex exhibits two pairs of doublets for the methylene protons.[11] The two faces of the oxacalix[3]arene macrocycle become inequivalent as a result of coordination of titanium out-of-plane of the three phenolic oxygen atoms. The presence of two sets of doublet pairs indicates that two different titanium complexes form during the reaction, in a ratio that varies from one batch to another. We postulate that the two complexes are the monomer [Ti(L)(O-*i*-Pr)] (**4a**) and the μ-isoproxo-bridged dimer [Ti(L)(μ-O-*i*-Pr)]$_2$ (**4b**), which are not in rapid equilibrium on the NMR time scale.

When THF is added to the NMR tube containing **4a** and **4b**, the spectrum simplifies to a single pair of doublets. The simplification of the spectrum could be due to rapid exchange between **4a** and **4b** in the presence of THF, or to the formation of a THF adduct, i.e. Ti(L)(O-*i*-Pr)(THF)$_n$ (n = 1, 2). Initially, one batch provided a 3:1 ratio of complexes **4a** and **4b** by ^{1}H NMR. After addition and removal of THF, the ratio had changed to 8.6:1. The reaction mixture became enriched in one of the isomers, possibly the monomer **4a**, as a result of the addition and removal of THF. Since the complexes **4a** and **4b** were reaction intermediates, no attempts were made to establish the nature of the mixture.

The mixture of **4a** and **4b** reacts with 2,4-pentanedione over

(11) ^{1}H NMR spectrum of **1** (R = *t*-Bu): ($CDCl_3$) δ 8.57 (s, 3H, phenolic OH), 7.13 (s, 6H, 3,5-aryl protons), 4.73 (s, 12H, methylene protons), and 1.24 (s, 27H, *t*-Bu protons). ^{13}C NMR spectrum of **1** (R = *t*-Bu): ^{13}C NMR (proton decoupled, $CDCl_3$) δ 153.47, 142.3, 126.85, 123.66, 71.69, 33.94, and 31.47. See refs 5–7.

1 h to form the acetylacetonate (acac) complex [Ti(L)(acac)] (**5**). Many attempts have been made to grow single crystals of complex **5**. Only microcrystals were isolated, and they were too small for an X-ray structure analysis.

Complex **5** has been characterized by ^{1}H and ^{13}C NMR, UV−visible, and FTIR spectroscopies, elemental analysis, and mass spectroscopy. Room temperature ^{1}H NMR spectra indicate a pair of doublets for the methylene protons and singlets for the aryl and *tert*-butyl protons on the macrocycle ligand. The acac ligand exhibits singlets for the methyl and methine protons. This spectrum is consistent with the presence of only one titanium complex. The yellow-orange color of complex **5** may be due to the ligand-to-metal charge transfer band at 338 nm which probably involves the phenoxide rings of the macrocycle. A similar phenoxide-to-titanium charge transfer has been proposed for the yellow-orange color of $Ti(OAr)_2(chelato)_2$ (chelato = 8-hydroxyquinolinate or 8-hydroxyquinaldinate) and $[Ti(OPh)Cl_2(\mu\text{-}OPh)]_2$.[12] Infrared spectra of complex **5** in the solid state and in solution exhibit bands at 1580 and 1589 cm^{-1}, respectively, which indicate that the acac ligand is chelating to titanium. Nonchelating acac ligands are reported to exhibit bands in the 1600−1750 cm^{-1} region due to the ketonic carbonyl group.[13] Elemental analysis (C, H, Ti) and mass spectral data are in excellent agreement with the proposed Ti(L)(acac) structure of the complex. FAB mass spectral analysis indicate a series of molecular ion peaks consistent with a mixture of (M^+) and $(M + H)^+$ molecular ions and with the presence of the isotopes of titanium (^{46}Ti, 8.0%; ^{47}Ti, 7.5%; ^{48}Ti, 73.7%; ^{49}Ti, 5.5%; ^{50}Ti, 5.3%) and carbon.

VT NMR Studies of Complex 5 and Computer Simulation of VT NMR Spectra. As the temperature is lowered, the NMR spectrum of **5** in CD_2Cl_2 gradually becomes more complex as shown by the series of spectra on the left side of Figures 1 and 2. The pair of doublets in the macrocycle methylene region gradually becomes six doublets (left side of Figure 1), and the acac methyl singlet splits into two singlets (left side of Figure 2). The 310 K spectrum in Figure 1 is consistent with the macrocycle possessing C_{3v} symmetry, where the top and bottom faces of the macrocycle are inequivalent, thus $O_1 = O_2 = O_3$, $H_A = H_B = H_C$, and $H_D = H_E = H_F$ (Chart 1). The low temperature spectrum is consistent with C_s symmetry where the macrocycle possesses a mirror plane that passes through O_1 and the oxygen of the opposite ether linkage, and $O_2 = O_3$, $O_1 \neq O_2$, $H_A \neq H_B \neq H_C$, and $H_D \neq H_E \neq H_F$ (Chart 1). No concentration dependence of the VT NMR spectra was observed with nearly a factor of 5 change in the concentration of **5**; thus, the exchange mechanism is not associative.

The ^{13}C NMR spectra of complex **5** also indicated C_{3v} macrocycle symmetry and equivalent acac methyl groups at high temperatures (298 K) and C_s macrocycle symmetry and inequivalent acac methyl groups at low temperatures (182 K). A minor reaction component (~5%) was present in the ^{13}C NMR spectra at 182 K. Only a few of the signals for this minor component were detectable from the noise in the base line. The acac carbonyl region consisted of two peaks, and the 1- and 4-aryl regions indicated three peaks for this minor species. This spectrum is consistent with the macrocycle ligand possessing no symmetry ($O_1 \neq O_2 \neq O_3$) and the acac methyl groups being inequivalent.

The asterisks in Figure 2 indicate ^{13}C satellites of the macrocycle *tert*-butyl groups, which are upfield (1.2 ppm, 300 Hz) of the acac methyl signals, and minor impurities in complex **5**. Although the asterisked peaks appear to increase in intensity and then decrease in intensity as the temperature is decreased, these changes are the result of the spectra not being normalized. If the spectra were scaled, the heights of the asterisked peaks would be identical. As the temperature is lowered, the acac methyl signals broaden and become less intense compared to the asterisked peaks. At the lowest temperature, the two singlets (3H integral each) have half the intensity of the room temperature singlet (6H integral). The decrease in signal to noise in the macrocycle methylene signals (Figure 1) is also a result of the broadened peaks in the intermediate exchange region and the significantly decreased intensity of the six low temperature doublets (2H integral each) compared to the high temperature doublets (6H integral each).

Table 1. Rate Constants for the Interconversion of the Macrocycle Methylene and Acac Methyl Regions Based on Schemes 1 and 2

T (K)	k_1 (s^{-1})[a]	k_2 (s^{-1})[b]	k_3 (s^{-1})[b]	k_4 (s^{-1})[c]	% minor[d]	k_2/k_1[a,b]	k_4/k_1[a,c]
196					4.0		
203		13.7		12.7	5.0		
211	7.0	24.5		35.0	6.0	3.5	5.0
218	18.2	65.1	1.50	79.2	10	3.6	4.4
225	38.4	123	5.00	162.6	14	3.2	4.2
232	91.1	237	14.0	351	15	2.6	3.9
239	221	460	63.0	656	16	2.1	3.0
246	411	897	195	1410	20	2.2	3.4
253	800	2000	411	3360	22	2.5	4.2
261	1450	4550	610	5550	23	3.1	3.8
268	3210	8290	936	8610		2.6	2.7
275	6050						

[a] See Scheme 1. [b] See Scheme 2B. [c] See Scheme 2C. [d] Percentage of minor component (±2%) of the total acac methyl signal.

Simulations of the exchange between the methylene protons in the macrocycle ligand and the acac methyl groups were performed independently, as discussed in the Experimental Section, and exchange rate constants were obtained as a function of temperature. The macrocycle methylene region was simulated using the two independent, three-site exchange processes shown in Scheme 1. The H_i and $H_{i'}$ sets of protons ($i = 1-3$) refer to the protons on the same face of the macrocycle which undergo exchange. No exchange is observed between the H_i and $H_{i'}$ protons, since the macrocycle methylene protons appear as a pair of doublets throughout the temperature region. In other words, it is not possible for the titanium center to move from one face of the macrocycle to the other face on the NMR time scale. The simulated spectra shown on the right side of Figure 1 indicate an excellent fit with the experimental spectra. Values for the rate constant k_1 (see Scheme 1) obtained from the simulations are listed in Table 1.

Inspection of Figure 2 reveals that a simple two-site exchange process (Scheme 2A) is inadequate in explaining (1) the differential broadening of the methyl resonances, (2) the unequal integrals for the two acac methyl signals in the low temperature spectra, and (3) the downfield shift of the high temperature (310 K) acac methyl singlet when compared to the midpoint between the low temperature (182 K) singlets. The differential broadening is especially evident in the 218 K spectrum (Figure 2). The unequal integrals for the signals in the low temperature spectra were not due to incomplete relaxation of the acac methyl protons, since increases in the relaxation delay up to 20 s had no effect on the integrals.

To explain the above behavior, we propose the existence of a minor isomer of complex **5** whose acac methyl signal (H_6) lies under the downfield acac signal of the major component (H_4). As discussed in the Experimental Section, two mechanisms were examined for the exchange in the acac methyl region

(12) (a) Harrod, J. F.; Taylor, K. R. *Inorg. Chem.* **1975**, *14*, 1541. (b) Watenpaugh, K.; Caughlan, C. N. *Inorg. Chem.* **1966**, *5*, 1782.

(13) (a) Lindmark, A. F.; Fay, R. C. *Inorg. Chem.* **1975**, *14*, 282 and references therein. (b) Saxena, U. B.; Rai, A. K.; Mathur, V. K.; Mehrotra, R. C. *J. Chem. Soc. A* **1970**, 904 and references therein.

Table 2. Activation Parameters for the Interconversion of the Macrocycle Methylene and Acac Methyl Regions

signal (k)	$\Delta H^{\ddagger}$ (kcal/mol)	$\Delta S^{\ddagger}$ (cal/K mol)	$\Delta G^{\ddagger}$ [a] (kcal/mol)
methylene (k_1)	11.5 ± 0.5	0.62 ± 2	11.3 ± 1
methyl (major) (k_2)	10.3 ± 0.5	−2.3 ± 2	11.0 ± 1
methyl (minor) (k_3)	15.2 ± 1	13.0 ± 4	11.3 ± 2
methyl (k_4)	10.6 ± 0.5	−0.74 ± 1	10.8 ± 1

[a] $\Delta G^{\ddagger}$ was calculated at 298 K.

between the major proton signals (H_4 and H_5) and the minor proton signal (H_6) as shown in parts B and C of Scheme 2. The ^{13}C NMR spectrum at low temperature (182 K) confirmed the presence of a minor reaction species.

The mechanism in Scheme 2B involves a direct exchange between the H_4 and H_5 protons with a rate constant k_2, and an exchange between the major isomer protons (H_4 and H_5) and the minor isomer proton signal (H_6) with a rate constant k_3. From simulations of this mechanism, the rate constants k_2 and k_3 were determined along with the population of the minor isomer, and these values are listed in Table 1. The ratios of the rate constants for the exchange of the acac methyl and macrocycle methylene protons (k_2/k_1) are observed to range from 2.1 to 3.6 with no obvious correlation to the temperature. The average value for the ratio k_2/k_1 is 2.8. The spectra on the right side of Figure 2 result from these simulations and exhibit a good fit with the experimental spectra.

In contrast to Scheme 2B, Scheme 2C allows for the equilibration of the acac methyl groups (H_4 and H_5) only through their conversion to the proton site (H_6) of the minor reaction component. No direct exchange between H_4 and H_5 occurs in this mechanism. Simulation of the spectra in Figure 2 using this mechanism and the populations of the minor isomer determined for Scheme 2B, provided the values for the rate constant k_4 shown in Table 1. The ratios of the rate constants for exchange of the acac methyl and macrocycle methylene protons (k_4/k_1) are observed to range from 2.7 to 5.0 with no obvious correlation with the temperature. The average value for the ratio k_4/k_1 is 3.8. The simulated spectra obtained for Scheme 2C were essentially identical to those shown in Figure 2 for the simulations of Scheme 2B.

The inclusion of a minor reaction component would be expected to complicate the ^1H NMR of not only the acac methyl region but also the macrocycle methylene region, since the minor isomer would have its own set of methylene signals. Considering the signal-to-noise ratio of the experimental spectra and the small amount of the minor isomer (~4%) at 182 K, the signals for this minor component could be in the base line. The ^{13}C NMR signals for the minor species at low temperatures suggest that the macrocycle may possess no symmetry. As a result, the ^1H NMR spectrum would be expected to consist of 12 doublets (1H each) for the macrocycle methylene region. The intensity of these doublets would be small compared to the doublets for the major isomer. The inclusion of a minor isomer in the modeling of the methylene region was not pursued.

The activation parameters listed in Table 2 were determined from the Eyring plots of the rate constants k_1, k_2, k_3, and k_4 shown in Figure 3. The plots of k_2 and k_3 indicate considerable curvature, however, the plots are within the experimental error for the data points. The plots of k_1 and k_4 were linear.

Discussion

Possible Structures for Complex 5. A number of groups have reported the isolation of $Ti(dik)X_3$ complexes that resemble complex **5**, where dik represents a substituted 1,3-diketonate

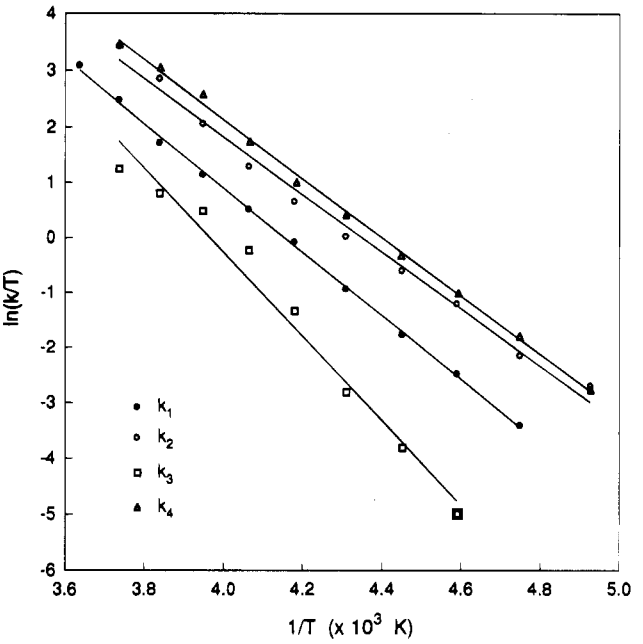

Figure 3. Eyring plots of rate constants for the macrocycle methylene and acac methyl exchange by Schemes 1 and 2.

and X = a halide or alkoxide ligand.[14] On the basis of solution molecular weight measurements, Mehrotra and Yamamoto and their co-workers have proposed that the sterically hindered alkoxide complexes $Ti(dik)(OR)_3$ (R = *i*-Pr and *s*-Bu) are monomeric and possess a five-coordinate structure. The complexes with smaller alkoxides (R = Me and Et) are proposed to be mixtures of the $Ti(dik)(OR)_3$ monomer and the $[Ti(dik)(OR)_2(\mu\text{-}OR)]_2$ dimer.[14g,h,i] The halide complexes $Ti(dik)X_3$ (X = Br, Cl, and F) are reported to dimerize to form a $[Ti(acac)(X)_2(\mu\text{-}X)]_2$ complex or to disproportionate into a mixture of TiX_4, and $Ti(dik)_2X_2$ complexes (eq 10). In the latter process, a $[Ti(dik)_2(\mu\text{-}X)_2TiX_4]$ dimer has been proposed as an intermediate.[14a-e] A crystal structure has been reported for the $[Ti(acac)(Cl)_2(\mu\text{-}Cl)]_2$ complex.[14b,c]

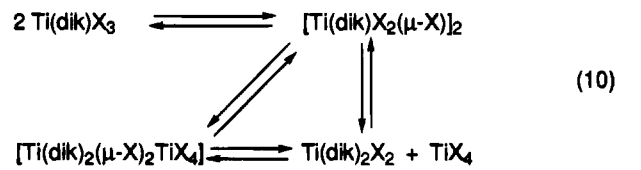

(10)

Alyea and Merrell have proposed trigonal bipyramidal structures for $Ti(chelato)(OR)_3$ complexes [chelato = *N,N,N'*-trimethyl-2-aminoethanamide and 2-(dimethylamino)ethoxide] which are structurally related to the $Ti(dik)X_3$ complexes. They observed that sterically bulky R groups resulted in five-coordinate, monomeric complexes.[15]

The mass spectral data for complex **5** indicate no evidence of the dimeric complexes $[Ti(L)(acac)]_2$ or $[Ti(L)_2Ti(acac)_2]$ (eq 10). Equilibration of the monomeric complex [Ti(acac)L] with

(14) (a) Somogyvari, A.; Serpone, N. *Can. J. Chem.* **1978**, *56*, 316. (b) Serpone, N.; Bird, P. H.; Somogyvari, A.; Bickley, D. G. *Inorg. Chem.* **1977**, *16*, 2381. (c) Serpone, N.; Bird, P. H.; Bickley, D. G. *J. Chem. Soc., Chem. Commun.* **1972**, 217. (d) Holloway, C. E.; Sentek, A. E. *Can. J. Chem.* **1971**, *49*, 519. (e) Thompson, D. W.; Rosser, R. W.; Barrett, P. B. *Inorg. Nucl. Chem. Lett.* **1971**, *7*, 931. (f) Thompson, D. W.; Somers, W. A.; Workman, M. O. *Inorg. Chem.* **1970**, *9*, 1252. (g) Puri, D. M.; Pande, K. C.; Mehrotra, R. C. *J. Less-Common Met.* **1962**, *4*, 393. (h) Puri, D. M.; Mehrotra, R. C. *J. Less-Common Met.* **1961**, *3*, 253. (i) Yamamoto, A.; Kambara, S. *J. Am. Chem. Soc.* **1957**, *79*, 4344.

(15) Alyea, E. C.; Merrell, P. H. *Inorg. Nucl. Chem. Lett.* **1973**, *9*, 69.

the dimers $[Ti(L)(acac)]_2$ or $[Ti(L)_2Ti(acac)_2]$ can be excluded as a mechanism for the isomerization of complex **5**, since the VT NMR spectra exhibited no concentration dependence.

Three possible structures have been considered for complex **5**: trigonal bipyramidal, tetragonal pyramidal, and octahedral. The trigonal bipyramidal structure is most consistent with the experimental data.

(I) Trigonal Bipyramidal Structure. One possible explanation for the variable temperature NMR spectra in Figures 1 and 2 could be that complex **5** possesses a trigonal bipyramidal (TBP) structure **6**, where the macrocycle oxygen atoms occupy two equatorial positions and one axial position and the acac ligand occupies an axial and an equatorial position. Evidence for a TBP Ti(IV) complex is provided by the crystal structure of the dimeric titanium complex, $[Ti(OPh)Cl_2(\mu\text{-}OPh)]_2$.[12b]

An alternative TBP isomer **7** is also possible, where two of the macrocycle oxygen atoms occupy the axial positions and one equatorial position, and the acac ligand occupies the remaining equatorial positions. On the basis of molecular models, isomer **7** is predicted to be significantly less stable than **6**, since the macrocycle ligand in **7** must distort to bridge the axial positions. The oval in structures **6** and **7** represents the trianion of macrocycle **1** (R = *t*-Bu).

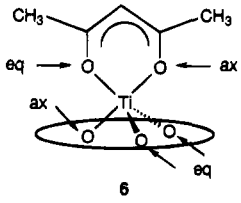

6

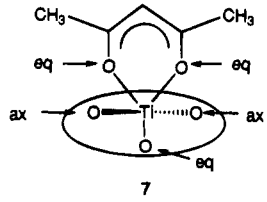

7

The VT NMR behavior observed for complex **5** can be explained by a rapid isomerization of the TBP isomer **6**. At high temperature, exchange between the axial and equatorial sites would result in equivalent acac methyl groups and a symmetric macrocycle on the NMR time scale. At low temperature, the acac methyl groups in **6** would be inequivalent, and the macrocycle would possess C_s symmetry ($O_2 = O_3$, $O_1 \neq O_2$, Chart 1).

(II) Tetragonal Pyramidal Structure. A tetragonal pyramidal (TP) structure was also considered as an alternative to the trigonal bipyramidal structures **6** and **7**. The TP structure is less likely than a TBP structure based on steric interactions in the d^0 complex **5**. The $[TiOCl_4]^{2-}$ anion is apparently the only square pyramidal Ti(IV) complex that has been reported.[16]

In order for a TP complex to explain the low temperature spectra, the macrocycle must occupy three of the four basal coordination sites. The acac ligand in this isomer would occupy the remaining basal site and the apical site and the acac methyl groups would be inequivalent. The macrocycle ligand in this isomer would span trans-coordination sites in the basal plane. This TP structure is predicted to be significantly less stable than the TBP structure **6** based on molecular models. The alternative and more stable TP isomer, where the macrocycle coordinates to two basal sites and one apical site, would possess equivalent acac methyl groups and cannot be responsible for the low temperature spectra. As a result, the TP structure was not further considered as a structure for complex **5**.

(III) Octahedral Structure. An alternative structure for complex **5** could be the octahedral structure **8** where two of the ether linkages of the macrocycle ligand coordinate to the titanium center and the acac ligand is nonchelating. The symmetry of **8** is consistent with the low temperature spectra of complex **5**, since the macrocycle possesses C_s symmetry and the acac methyl groups are inequivalent. The alternative octahedral complex **9** that has only one coordinating macrocycle ether linkage and a chelating acac ligand, would have the correct low temperature C_s symmetry of the macrocycle, but it would only have a single acac methyl resonance. The solution and solid state IR spectra are inconsistent with complex **5** possessing a nonchelating acac ligand, since no bands are observed in the region typically assigned to the ketonic group of a nonchelating acac ligand.[13] As a result, the octahedral complexes **8** and **9** were not considered as possible structures for complex **5**. The macrocycle ligand in complexes **8** and **9**, occupies a face of the octahedral complex. Meridonal coordination of the macrocycle ligand seems unlikely based on molecular models, since the macrocycle ligand must distort to span the trans-coordination sites.

Table 3. Proposed Mechanisms for the Isomerization of Complex **5**

Mechanism		Rate Constants	R_{theor}[c]	R_{exp}[c]
I) Trigonal Bipyramidal Isomerization via TR Processes[a]				
6 $\rightleftharpoons$ 6 (k_{ex}, k_{ex})	TR_1	$k_1 = k_{ex}/2$, $k_2 = k_{ex}$	2.0	2.8[a]
minor species (7, 9)	TR_2	$k_1 = k_{ex}/2$, $k_2 = 0$	0	2.8[a]
	TR_3	$k_1 = 0$, $k_2 = k_{ex}$	∞	2.8[a]
II) Trigonal Bipyramidal Isomerization via BP Processes[a,b]				
6 $\rightleftharpoons$ 6 (k_M, k_M)	BP_M	$k_1 = k_M/2$, $k_2 = k_M$	2.0	2.8[a]
7 (k_{-m}, k_m, k_{-m}, k_m)	BP_m	$k_1 = k_m/4$, $k_2 = k_m/2$	2.0	3.8[b]
III) Trigonal Bipyramidal-Tetrahedral Isomerization[b]				
6 $\rightleftharpoons$ 12 $\rightleftharpoons$ 6 (k_{ex}, k_{-ex}, k_{-ex}, k_{ex})		$k_1 = k_{ex}/3$, $k_4 = k_{ex}/2$	1.5	3.8[b]

[a] Scheme 2B, see text. [b] Scheme 2C, see text. [c] R_{theor} and R_{exp} are the theoretical and experimental ratios of the rate constants for exchange of the macrocycle methylene and acac methyl protons (k_2/k_1 and k_4/k_1 for mechanisms that fit Schemes 2B and 2C, respectively).

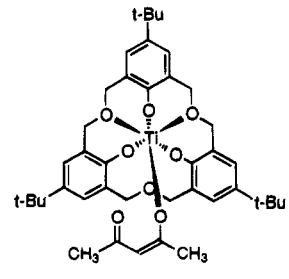

8

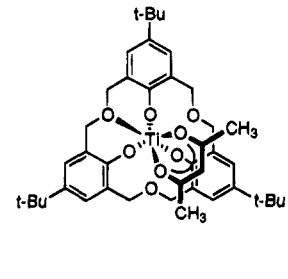

9

Proposed Mechanisms for the Dynamic ^1H NMR Behavior. Table 3 lists three potential mechanisms which we have considered for the isomerization of the putative trigonal bipyramidal complex **5**.

(I) Isomerization via a Turnstile Rotation. The isomerization of a TBP isomer **6** could occur by either turnstile rotation (TR) or Berry pseudorotation (BP) processes. Both of these mechanisms have been proposed for the isomerization of trigonal bipyramidal phosphoranes.[17,18] Theoretical studies indicate that the pseudorotation mechanism is a lower energy pathway than

(16) Felta, A. *Z. Chem.* **1967**, *7*, 158.

the turnstile rotation mechanism.[17a,19] In contrast to the BP process, a TR process requires very little distortion of the macrocycle ligand. Ramirez and Ugi and their co-workers have studied a caged oxyphosphorane possessing *cis*-1,3,5-cyclohexanetriol as three of its five ligands and have proposed that this compound can only isomerize by a turnstile rotation because of the rigid, cagelike structure of the oxyphosphorane.[17b-d]

In the TR mechanism (Mechanism I, Table 3), an equatorial and an axial ligand rotate together as a "duo" while the remaining two equatorial ligands and one axial ligand rotate as a "trio" in the opposite direction. In addition to the rotation of the duo and trio in opposite directions, the bond angles between the ligands change during the rotation. This mechanism is depicted in **10** where the acac ligand (O_4 and O_5) acts as the duo and the macrocycle (O_1, O_2, and O_3) acts as the trio.

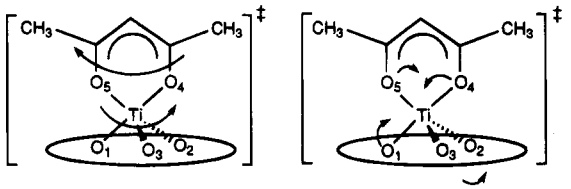

10 **11**

Since this mechanism allows for the direct isomerization of the major species, it is consistent with Scheme 2B for the acac methyl region. The minor species required in Scheme 2B could be the less stable trigonal bipyramidal isomer **7** or the octahedral complex **9**. The TBP isomer **7** could form from **6** via a TR process where the trio includes the axial acac oxygen (O_4), and the two equatorial macrocycle oxygens (O_2 and O_3). The octahedral species **9** could form from the TBP complex **6** by coordination of a macrocycle ether linkage. Complex **9** appears most consistent with the experimental observations for the minor species. A small distortion of **9** could result in asymmetric macrocycle and acac ligands as observed for the minor species by low temperature ^{13}C NMR.

Depending on the degree of rotation of the duo with respect to the trio, the macrocycle methylene protons and the acac methyl groups can either exchange or remain unchanged. Five rotational processes are possible which will be abbreviated TR_n ($n = 1-5$) for rotations of the duo $60(n)°$ with respect to the trio.

For a TR_1 process, the macrocycle protons and the acac methyl groups exchange equatorial and axial positions. If k_{ex} is the rate constant for a TR_1 process, then the rate constant k_2 in Scheme 2B can be expressed as $k_2 = k_{ex}$, since each 60° rotation results in the exchange of the acac methyl groups. The rate constant k_1 in Scheme 1 represents the rate constant for conversion of a H_1 proton to a H_2 proton. A TR_1 process results in the conversion of only one of the two H_1 protons to a H_2 proton. The other H_1 proton is converted to a H_3 proton. As a result, the rate constant k_1 can be expressed as $k_1 = k_{ex}/2$. The ratio of acac and macrocycle exchange rate constants (k_2/k_1) for a TR_1 process is predicted to be 2.

For a TR_2 process, only the macrocycle protons exchange positions and the acac methyl groups remain in their original positions ($k_2 = 0$). In contrast, a TR_3 process results in the exchange of the acac methyl groups without any change in the position of the macrocycle ligand ($k_1 = 0$). The relationship between the TR_2 rate constant (k_{ex}) and k_1 is identical to a TR_1 process ($k_1 = k_{ex}$); thus, the predicted rate constant ratio (k_2/k_1) would be zero. The ratio of rate constants for a TR_3 process (k_2/k_1) would be predicted to be infinitely large since $k_1 = 0$. TR_4 and TR_5 processes have the same effect on the acac and macrocycle ligands as TR_2 and TR_1 processes, respectively.

The k_2/k_1 ratios indicate that none of the TR_n processes provide the experimental result that $k_2/k_1 = 2.8$ (Scheme 2B). The TR_1 process is, however, fairly close to the experimental ratio. If all three processes were occurring simultaneously, in particular TR_1 and TR_3 processes, then a ratio of 2.8 could be possible.

(II) Isomerization via Berry Pseudorotation Processes. During a BP process (Mechanism II, Table 3), two axial groups move toward the midpoint of two equatorial groups, and at the same time, the two equatorial groups move in their plane toward the third equatorial group. The equatorial group which does not move is referred to as the "pivot" for the BP process.[18]

The BP isomerization of complex **5** is shown in **11**, where the equatorial acac oxygen (O_2) acts as the pivot for the pseudorotation. If one of the equatorial macrocycle oxygens were taken as the pivot (O_2 or O_3), then the less stable TBP isomer **7** would be formed. The BP process shown in **11** results in the direct isomerization of the major isomer **6**, thus this BP_M mechanism (Table 3) would fit Scheme 2B. The BP_M process has the same net effect on the macrocycle and acac groups as a TR_1 process. As a result, the anticipated rate constant ratio (k_2/k_1) would be 2.0 which is close to the experimental ratio of 2.8.

If the isomerization occurred only via the less stable TBP isomer **7** (process BP_m), then the mechanism would fit Scheme 2C. Return to **6** from **7** using the equatorial macrocycle oxygen in **7** as the pivot would result in the macrocycle occupying all three equatorial sites and the acac ligand spanning the axial sites. This geometry is not possible for the acac ligand. Thus, return to **6** from the intermediate **7** could only occur using the equatorial acac oxygens as pivots, and there would be a 50% probability of exchange of the acac methyl groups ($k_4 = k_m/2$) and the macrocycle ligand. Since only one of the two H_1 protons in **6** would be converted to a H_2 proton if exchange occurred, the rate constant relationship would be $k_1 = k_m/4$. The theoretical ratio of rate constants for a BP_m process (k_4/k_1) is 2, which is in contrast with the predicted value of 3.8 in Scheme 2C. We believe that the BP_M or BP_m mechanisms are both unlikely, since they require considerable flexibility of the macrocycle ligand.

(III) Isomerization via a Tetrahedral Intermediate. The interconversion between TBP complex **6** and the tetrahedral intermediate **12** possessing a nonchelating acac ligand was also examined as a mechanism for the isomerization of complex **5** (Mechanism III, Table 3). Interconversion between a chelating and nonchelating acac ligand has been proposed for the isomerization of main group acetylacetonate complexes.[20] This mechanism would fit Scheme 2C, since exchange of the

(17) (a) Ugi, I.; Marquarding, D.; Klusacek, H.; Gillespie, P. *Acc. Chem. Res.* **1971**, *4*, 288. (b) Ugi, I.; Marquarding, D.; Klusacek, H.; Gokel, G.; Gillespie, P. *Angew. Chem., Int. Ed. Engl.* **1970**, *9*, 703. (c) Ramirez, F. ; Ugi, I. *Bull. Chim. Soc. Fr.* **1974**, 453. (d) Ramirez, F.; Ugi, I.; Lin, F.; Pfohl, S.; Hoffman, P.; Marquarding, D. *Tetrahedron* **1974**, *30*, 371.

(18) (a) Berry, R. S. *J. Chem. Phys.* **1960**, *32*, 933. (b) Sheline, R. K.; Mahnke, H. *Angew. Chem., Int. Ed. Engl.* **1975**, *14*, 314. (c) Meakin, P.; Jesson, J. P. *J. Am. Chem. Soc.* **1973**, *95*, 7272.

(19) (a) Hoffmann, R. H.; Howell, J. M.; Muetterties, E. L. *J. Am. Chem. Soc.* **1972**, *94*, 3047. (b) Strich, A. *Inorg. Chem.* **1978**, *17*, 942 and references therein. (c) Altmann, J. A.; Yates, K.; Csizmadia, I. G. *J. Am. Chem. Soc.* **1976**, *98*, 1450.

(20) (a) Faller, J. W.; Davison, A. *Inorg. Chem.* **1967**, *6*, 182. (b) Kawaguchi, S. *Variety in Coordination Modes of Ligands in Metal Complexes*, Inorganic Chemistry Concepts 11; Springer-Verlag: Berlin, 1988; Chapter 5 and references therein.

macrocycle and acac positions must proceed via the formation of **12**. Intermediate **12** possesses inequivalent acac methyl groups and a symmetric macrocycle. The symmetry of **12** is inconsistent with the ^{13}C NMR signals for the minor species at low temperatures.

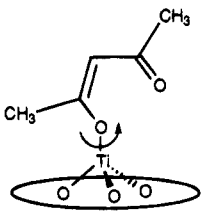

12

The process of converting **6** to **12** back to **6** could result in either exchange or return of the acac and the macrocycle protons back to their original positions. The rate constant for the formation of **12** (k_{Td}) can be related to k_4 as $k_4 = k_{Td}/2$, since the acac methyl groups have an equal probability of exchanging or remaining unchanged. Similarly, the two H_1 protons on the macrocycle ligand in **6** could either return to their original positions on returning to **6** from **12**, or they could be converted to one H_2 proton and one H_3 proton. There are two ways to return to **6** from **12** that result in exchange, and only one way that results in return to **6** without exchange. As a result, each conversion of **6** to **12** back to **6** results in a one-third probability that proton H_1 is converted to proton H_2; thus, $k_1 = k_{Td}/3$. The ratio of rate constants for this mechanism (k_4/k_1) is predicted to be 1.5, in contrast with the value of 3.8 calculated for Scheme 2C. We believe that this mechanism is not responsible for the dynamic isomerization of complex **5**, since it cannot explain the substantially larger rate constant ratio for Scheme 2C.

Conclusions

In this paper, we have examined the coordination of the oxacalix[3]arene macrocycles **1** to Ti(IV). One of the complexes, the Ti(L)(acac) complex **5**, is proposed to possess a trigonal bipyramidal structure **6** based on ^1H and ^{13}C NMR and FTIR spectra. Complex **5** exhibits a dynamic behavior which we believe is due to a rapid exchange of the axial and equatorial positions in **6** on the NMR time scale. Three mechanisms were considered for the isomerization of the putative trigonal bipyramidal complex **5**. Only the turnstile rotation mechanism can adequately explain the observed relative rates of exchange of the macrocycle and acac methyl protons. The low activation enthalpies and small activation entropies obtained for the isomerization of complex **5** are consistent with either the turnstile rotation or Berry pseudorotation mechanisms, since both mechanisms require only an intramolecular rearrangement process without any bond cleavage. Further mechanistic studies are needed to probe the mechanism of the dynamic behavior for this complex.

Acknowledgement is made to the donors of the Petroleum Research Fund, administered by the American Chemical Society, for partial support of this research. Sandia National Laboratories are also acknowledged for financial support of this research through the Sandia-University Research Program. FAB mass spectral analysis was performed at the Midwest Center for Mass Spectrometry with partial support by the National Science Foundation, Biology Division (Grant No. DIR9017262). M.R. would like to acknowledge support from the National Science Foundation-Research Experiences for Undergraduates Program. The NSF Chemical Instrumentation Program is acknowledged for providing a low field NMR spectrometer.

Supplementary Material Available: Kinetic matrices used in the computer simulation of the mechanisms in Schemes 1 and 2 (1 page). Ordering information is given on any current masthead page.